Modulation of Dimerization, Binding, Stability, and Folding by Mutation of the Neurophysin Subunit Interface†

Sharon Eubanks,‡ Tam L. Nguyen,‡ David Peyton,§ and Esther Breslow*,‡

Department of Biochemistry, The Joan and Sanford I. Weill Medical College of Cornell University, 1300 York Avenue, New York, New York 10021, and Department of Chemistry, Portland State University, Portland, Oregon 97207-0751

Received January 24, 2000; Revised Manuscript Received April 3, 2000

ABSTRACT: Bovine neurophysins, which have typically served as the paradigm for neurophysin behavior, are metastable in their disulfide-paired folded state and require ligand stabilization for efficient folding from the reduced state. Studies of unliganded porcine neurophysin (oxytocin-associated class) demonstrated that its dimerization constant is more than 90-fold greater than that of the corresponding bovine protein at neutral pH and showed that the increased dimerization constant is accompanied by an increase in stability sufficient to allow efficient folding of the reduced protein in the absence of ligand peptide. Using site-specific mutagenesis of the bovine protein and expression in *Escherichia coli*, the functional differences between the bovine and porcine proteins were shown to be attributable solely to two subunit interface mutations in the porcine protein, His to Arg at position 80 and Glu to Phe at position 81. Mutation of His-80 alone to Arg had a relatively small impact on dimerization, while mutation to either Glu or Asp markedly reduced dimerization in the unliganded state, albeit with apparent retention of the positive linkage between dimerization and binding. Comparison of the peptide-binding constants of the different mutants additionally indicated that substitution of His-80 led to modifications in binding affinity and specificity that were independent of effects on dimerization. The results demonstrate the importance of the carboxyl domain segment of the subunit interface in modulating neurophysin properties and suggest a specific contribution of the energetics of ligand-induced conformational change in this region to the overall thermodynamics of binding. The potential utility to future studies of the self-folding and monomeric mutants generated by altering the interface is noted.

Protein self-association and its modulation by ligands play a central role in many biological processes. Bovine neurophysin was probably the first protein for which ligand-facilitated dimerization was reported (*1*, *2*). The unliganded protein is in monomer−dimer equilibrium in the absence of hormone or related peptide, and the equilibrium is driven to the right by binding of ligand to the hormone-binding site. Molecular mechanisms underlying this effect are not known, but the crystal structures of neurophysin (NP)[1] complexes (Figure 1) indicate that the monomer−monomer interface and the hormone-binding site are separate from each other (*3*, *4*). A complete understanding of this effect requires knowledge of the structures not only of liganded and unliganded dimers, but also of the monomeric state. Two crystal structures have been reported for the liganded dimeric state (*3*, *4*), and one is being refined for the unliganded dimer (*5*), but the monomeric state has so far been unavailable.

Self-association is thought to play an important role in the intracellular targeting of the common precursors of the neurophysins and their associated peptide hormones, oxytocin and vasopressin, to regulated neurosecretory granules (e.g., refs *6*, *7*). However, whether dimerization alone or higher-order self-association processes are essential and whether there is a role for hormone in targeting beyond its effects on dimerization have not been unambiguously untangled (see Discussion). Ambiguity as to the role of hormone arises in part because of the behavior of the bovine neurophysins, which require hormone binding for efficient folding (*8*) and, hence, for normal protein self-association.

Factors governing intersubunit recognition in this system are unclear. Dimerization principally involves β-sheet interactions between residues 32−37 of the amino-terminal domains of the two interacting subunits and between residues 77−81 of the carboxyl-terminal domains (Figure 1). The amino-terminal interface segment is strongly conserved among different neurophysins, but the carboxyl domain segment exhibits significant variation (*6*, *9*). In bovine NP (Figure 2), this variation includes the change from Val and Thr at positions 80 and 81, respectively, in BNP-II (bovine vasopressin-associated NP) to the more hydrophilic His and

† Supported by NIH Grant GM-17528 and NIH Fellowship F31 NS-10204 to S.E.

* Corresponding author. Telephone: (212)-746-6428. Fax: (212)-746-8329. E-Mail: ebreslow@mail.med.cornell.edu.

‡ The Joan and Sanford I. Weill Medical College of Cornell University.

§ Portland State University.

[1] Abbreviations: NP, neurophysin; BNP-I, bovine oxytocin-associated NP; PNP-II, porcine oxytocin-associated NP; BNP-II, bovine vasopressin-associated NP; RF, RE, DE, and EE, mutants of BNP-I, containing the sequences RF, RE, DE, and EE, respectively, at residues 80, 81; Phe-PheNH$_2$, L-phenylalanyl-L-phenylalanine amide; Phe-TyrNH$_2$, L-phenylalanyl-L-tyrosine amide; Abu-TyrNH$_2$, L-α-aminobutyryl-L-tyrosine amide; Mes, 2-[*N*-morpholino]ethanesulfonic acid; CD, circular dichroism; NMR, nuclear magnetic resonance; $\bar{\nu}$, number of peptide molecules bound per NP subunit.

10.1021/bi0001527 CCC: $19.00
Published on Web 06/16/2000

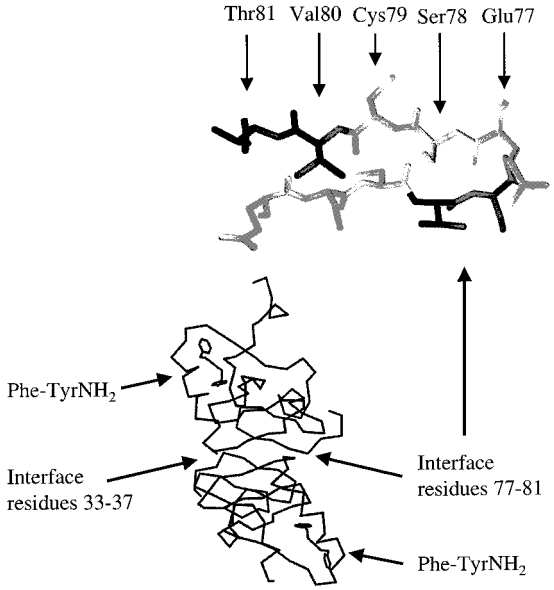

FIGURE 1: α-Carbon map of a dimer of BNP-II complexed with the peptide *p*-iodo-L-phenylalanyl-L-tyrosine amide, showing the relationship between the peptide-binding site and the subunit interface. The iodo group is omitted for simplification. An expanded stick-model representation of interactions of residues 77−81 across the interface is also shown. Residues 80 and 81 are in bold. The side chains of both residues contact the carbonyl oxygen of Glu-77, and the Thr-81 side chain additionally contacts the Glu-77 side chain. (Drawn from the structure 2bn2 in the Protein Data Bank.)

```
                    10                  20                  30
BNP-I   AVLDLDVRTCLPCGPGGKGRCFGPSICCGDELGCF
PNP-II  ----------K----------
BNP-II  --MS------E L--- Q----------

                40                  50                  60                  70
BNP-I   VGTAEALRCQEENYLPSPCQSGQKPCGSGGRCAAA
PNP-II  ----------E----------
BNP-II  ----------

                    80                  90
BNP-I   GICC SPDGCHEDPACDPE AAFSQ
PNP-II  ----------N----------RF----------T-------
BNP-II  ----------NDES---VTEPE---REGIVG---PRRV
```

FIGURE 2: Amino acid sequences of BNP-I, NP-II, and PNP-II (*9*). Note that residue 92 of BNP-I is the terminal residue in the expressed protein (*18*) and in most BNP-I preparations isolated from pituitary gland preparations. Sequences of PNP-II and BNP-II are shown where they differ from that of BNP-I. Residues 80−81 are underlined.

Glu, respectively, in BNP-I (bovine oxytocin-associated NP), with only a modest impact on dimerization at pH 6 (*2*). Additionally, mixed dimers with affinities characteristic of their formation of homodimers form between the two bovine NPs (*10*). While this might suggest that the side chains of the carboxyl domain interface are not direct participants in self-association, NMR and chemical-modification studies suggest participation of the His-80 side chain of BNP-I (*11*), and intersubunit interactions involving the side chains of BNP-II residues 80 and 81 are evident crystallographically (Figure 1). Of particular interest to us was the suggestion from earlier gel-filtration studies that porcine oxytocin-associated NP (PNP-II), which differs from its bovine counterpart at residues 80 and 81 and at four other positions (Figure 2), self-associates significantly more strongly in the unliganded state than does bovine NP (*12*, *13*).

This study represents further investigation of the increased self-association of porcine oxytocin-associated NP, the basis of this increase, and the effect of this on other NP properties. The results are shown to allow the design of neurophysins with reduced dimerization constants, which should facilitate structural studies of the monomeric state, and the design of neurophysins with increased dimerization constants, which are shown to allow separation of the process of folding from that of ligand binding. Additionally, they provide evidence for a modulating role of the subunit interface in ligand-binding thermodynamics.

MATERIALS AND METHODS

Preparation of Bovine and Porcine Oxytocin-Associated Neurophysins from Posterior Pituitary Lobes. BNP-I was prepared from bovine posterior pituitary lobes as described elsewhere (*14*) and additionally purified by affinity chromatography (*15*). PNP-II was prepared from lyophilized porcine posterior pituitary lobes supplied by Pel-Freez. The lobes were homogenized in cold 0.1 N HCl, and the resulting suspension was stirred overnight in the cold. Following centrifugation at 4 °C, the supernatant was collected and stored in the cold, while the pellet was resuspended in cold 0.1 N HCl, rehomogenized, and again allowed to stir overnight in the cold. The suspension was recentrifuged, and the combined supernatants from the two extractions were further purified to yield the crude hormone−NP complexes as described for HCl extracts of bovine posterior pituitary acetone powder (*16*). NP components were then separated from hormone by gel filtration on Sephadex G-75 in 0.1 M formic acid, a procedure that also gave partial separation of PNP-II from the vasopressin-associated porcine neurophysins PNP-I and -III (*12*) because of its stronger self-association. Lyophilized fractions containing PNP-II were then subjected to affinity chromatography (*15*) to remove contaminating foreign proteins and denatured NP. The resultant binding-competent protein was fractionated into its individual NP components by reverse-phase HPLC on a Vydak C-18 column using a gradient beginning with 80% solvent A (0.1% TFA in H_2O) and 20% solvent B (0.1% TFA in CH_3CN) and ending with 60% A and 40% B at 40 min. This procedure also separated PNP-II into three components, representing residues 1−93, 1−92, and 1−91, respectively, in order of their elution. These components were used interchangeably because BNP-I, which is similarly heterogeneous at its carboxyl terminus, was not similarly fractionated and because there is no evidence of a role for these carboxyl-terminal residues (*17*).

Preparation of Recombinant Neurophysins. The preparation of recombinant bovine oxytocin-neurophysin precursor has been described earlier (*18*); the precursor is expressed in *Escherichia coli* as a fusion protein in which the precursor sequence is preceded by a His tag and the TrpLe leader sequence. The cDNA sequence encoding the oxytocin-Gly-Lys-Arg segment of the precursor was removed by mutagenesis using Stratagene kits, the structure of the product cDNA was confirmed by sequencing (Cornell University Sequencing Facility), and the resultant fusion protein encoding BNP-I

was expressed and cleaved by CNBr as previously described. The protein segment representing unfolded BNP-I [oxidized state containing mispaired disulfides (*18*)] was collected from the wash and flow-through fractions of a Ni-NTA column and was dialyzed against 0.1 M acetic acid. Protein was folded at pH 8.0 (pH adjusted with Tris base) at a concentration of ~1 mg/mL in the presence of 10 mM Phe-TyrNH$_2$ and 0.1 mM EDTA with 1.5 mM β-mercaptoethanol added as a disulfide rearrangement agent. The protein was allowed to stand under these conditions for several hours at room temperature and then was stirred in air for a total period of 24−48 h. The protein was separated from peptide and other reagents by gel filtration in 0.2 M acetic acid and was lyophilized. Folded protein was separated from unfolded protein by affinity chromatography (*15*), dialyzed against 0.1 M acetic acid, and lyophilized. The identity of the folded protein was confirmed by mass spectrometry (Weill Medical College Mass Spectrometry Facility) and its characteristic CD and peptide-binding behavior (*6*). As with expression of the precursor, yields were limited by covalent damage to the protein during expression and/or purification (*18*), but in this case, all folding-competent protein was efficiently folded, as was expected from earlier work (*8*). Yields of purified folded protein averaged 6 mg/L of growth medium.

The following variants of the wild-type protein were prepared by site-directed mutagenesis (Stratagene), representing mutations at position 80 and in one case also at position 81. The 80−81 sequence is His-Glu in BNP-I and was mutated to Arg-Glu (the RE mutant), Arg-Phe (the RF mutant), Glu-Glu (the EE mutant), and Asp-Glu (the DE mutant). Purification and folding proceeded as for the native protein. Primary structures were confirmed by plasmid cDNA sequencing and the electrophoretic and NMR properties of the folded products.

CD Spectroscopy. CD spectra were obtained on a Jasco J-710 spectropolarimeter.

Analytical Ultracentrifugation. Molecular weights of PNP-II and the RF mutant of BNP-I were determined by equilibrium sedimentation at pH 6.2 (in 0.1 M ammonium acetate, 2 mM Mes buffer) and 20 °C using a Beckman model XL-A analytical ultracentrifuge. A partial specific volume of 0.71, derived from amino acid composition, was used for molecular weight calculations.

NMR Spectroscopy and Its Application to the Determination of Dimerization Constants. Proton NMR studies were conducted at 600 and 400 MHz using procedures described earlier (e.g., ref *19*). pH meter readings in D_2O are uncorrected for isotope effects. The application of NMR spectroscopy to the determination of dimerization constants has been described elsewhere (e.g., ref *20*). Dimerization constants are most directly determined by monitoring, as a function of protein concentration, the relative intensities of signals near 6.2 and 6.4 ppm. These signals have been assigned in BNP-I by chemical exchange methods to the same proton in the monomer and dimer, respectively (*11*, *19*). Analogous studies confirm this assignment for the mutants as well. Where ambiguities exist, the intensity of the 6.4 ppm signal or of a dimer Phe proton signal at ~7.55 ppm relative to that of the signal from the 3,5-ring protons of Tyr-49 can also be used (*20*) in addition to less-quantitative information from dimerization-sensitive signals in the upfield aliphatic region of the spectrum (see Results).

Table 1: Dimerization Constants of BNP-I, PNP-II, and Mutant Neurophysins[a]

protein	pH	solvent	K (M^{-1})
BNP-I	6.2	D_2O[b,c]	1×10^4
BNP-I	6.1	D_2O	3×10^3
BNP-I	8.0−10.0	D_2O	$\sim 5 \times 10^2$
BNP-I[d]	3.5	D_2O[b]	7×10^5
PNP-II[e]	6.2	H_2O[c]	$\geq 9 \times 10^5$
RF mutant[e]	6.2	H_2O[c]	$\geq 3.5 \times 10^6$
RE mutant	6.4	D_2O	$\sim 1 \times 10^4$
DE mutant	6.2	D_2O	6×10^2
DE mutant	6.2	D_2O[c]	6×10^2
EE mutant	6.2	D_2O[c]	1×10^3
EE mutant	6.7	D_2O[c]	2×10^2
EE mutant	6.1	90% H_2O/10% D_2O	2×10^3
EE mutant	6.9	90% H_2O/10% D_2O	1×10^2
EE mutant	7.5	90% H_2O/10% D_2O	$< 1 \times 10^2$

[a] Determined by NMR at 25 °C from the relative intensity of signals at 6.2 ppm (monomer) and 6.4 ppm (dimer), as described elsewhere (*20*) unless otherwise noted. NMR values are reported to one significant figure. Studies were conducted in the absence of added salt unless otherwise noted by solvent footnote. [b] Represents studies in 0.1 M sodium phosphate. [c] Represents studies in 0.1 M ammonium acetate. [d] Data are from ref *21*. [e] Ultracentrifuge studies at 20 °C.

Dimerization constants of BNP-II measured in this manner at both neutral and low pH are within a few percent of values obtained by analytical ultracentrifugation under related conditions (cf., refs *2*, *20*, *21*). For BNP-I, comparison of dimerization constants obtained by NMR with those obtained by other methods is complicated by large pH effects on BNP-I dimerization that appear to be affected by ionic strength and/or buffer and the fact that these conditions differ in different studies (e.g., ref 22). Nontheless, the value 1×10^4 M^{-1}, obtained here for BNP-I dimerization at pH 6.2 in 0.1 M ammonium acetate/D_2O (Table 1), compares reasonably with values of $0.8-1.1 \times 10^4$ M^{-1} obtained by analytical ultracentrifugation and gel filtration at pH 5.6 in various acetate buffer systems in H_2O (*2*, *22*). Because of the effects of pH and buffer, examples of dimerization constants obtained under different conditions are provided in Table 1. Unless otherwise indicated, dimerization constants used in the analyses of binding and stability data were obtained under conditions of pH and buffer analogous to those used for the binding and stability measurements. Note that we have not observed significant differences between results in D_2O and H_2O that are attributable to isotope alone, but we cannot strictly preclude such potential effects.

Denaturation Studies. Stabilities of the folded proteins to denaturation by guanidine hydrochloride were determined as described earlier by monitoring CD spectra in the near-ultraviolet (*18*) range. Specific conditions of pH and buffer are indicated in the legend to Table 2. A 0.5 cm light path was utilized except for studies at 0.005 mM protein concentration, which were carried out using a 5 cm path.

Calculations of Predicted Effects of Dimerization on Stability. The total free energy of dimer denaturation can be viewed as the sum of the energies of dissociating the dimer to monomers plus the energy of unfolding the resulting monomers (*23*). Accordingly, estimates of the impact on stability of a change in dimerization constant involved consideration of the resultant change in the free energy of dimer dissociation in the absence of denaturant under the conditions of pH and protein concentration used in the experiment. For calculation of the free energy of the dimer

Table 2: Stability Parameters of Native and Mutant Neurophysins as Estimated from Guanidine Denaturation Studies at 25 °C[a]

protein	pH	m (kcal/mol M^{-1})	$\Delta G°$ (kcal/mol)
BNP-I[b] (0.1 mM)	8.0	1.0	3.0 (±0.3)
PNP-II[b] (0.08 mM)	8.0	1.3	6.4 (±0.5)
BNP-I[b] (0.05 mM)[c]	8.0	1.1	3.0 (±0.3)
BNP-I[b] (0.005 mM)	6.0	0.8	2.1 (±0.1)
BNP-I[b] (0.05 mM)[c]	6.0	1.1	3.0 (±0.1)
BNP-I (0.1 mM)	6.0	1.2	3.6 (±0.1)
BNP-I[b] (1.0 mM)	6.0	1.4	4.6 (±0.2)
RF mutant (0.1 mM)	6.0	1.4	6.4 (±0.4)
EE mutant (0.1 mM)	6.0	0.9	2.6 (±0)
BNP-I[b] (0.1 mM)[d]	3.5	1.1	2.7 (±0.2)
PNP-II[b] (0.1 mM)[d]	3.5	1.3	5.4 (±0.5)
RF mutant (0.1 mM)[d]	3.5	1.3	5.0 (±0.2)

[a] Samples are the recombinant proteins and were studied in 0.2 M ammonium acetate unless otherwise specified. $\Delta G°$ is the calculated standard free energy of unfolding in the absence of guanidine; values of m represent the change in the free energy of unfolding with change in guanidine concentration (*34*). [b] Purified from animal source. [c] 0.1 M ammonium acetate. [d] 0.1 M sodium phosphate buffer.

dissociation (ΔG_{dissoc}), dissociation to the native monomer was assumed. That is, ΔG_{dissoc} was calculated as the free energy associated with converting the equilibrium mixture of monomer and dimer in the absence of guanidine to all native monomer as follows:

$$\Delta G_{dissoc} = -\Delta G°_{dimerization} + RT \ln(M_{total})^2/(D_{equilibrium}) \quad (1)$$

where M_{total} is the final molar concentration of monomer (equal to the total molar concentration of NP subunits), $D_{equilibrium}$ is the initial equilibrium molar concentration of dimer, $\Delta G°_{dimerization}$ is the standard free energy of dimerization, and $-\Delta G°_{dimerization}$ is the standard free energy of dimer dissociation. The dimerization constants used for this calculation at pH 6.0 were those obtained at pH 6.2 because the values obtained here at pH 6.2 for BNP-I did not differ significantly from those obtained at pH 5.6 by other methods (vide supra).

Studies of Refolding from the Reduced State. Fully reduced proteins were prepared as described elsewhere (*18*) and refolded at room temperature by stirring in air at pH 8 (0.1 M Tris-acetate buffer with 1 mM β-mercaptoethanol and 0.1 mM EDTA), in either the absence or presence of 10 mM Phe-TyrNH$_2$ as indicated.

Binding Studies. Binding affinities for peptides known to bind to the hormone-binding site and to affect dimerization in a manner similar to the hormones (*6*) were determined either by fluorescence using affinity-purified unmodified protein or by CD using protein mononitrated at Tyr-49, both techniques as described elsewhere (*24*, *25*). All studies were conducted at pH 6.2, 25 °C, and in 0.1 M ammonium acetate containing 2 mM Mes. CD studies utilized Phe-PheNH$_2$ or Abu-TyrNH$_2$, as indicated in the text; fluorescence binding studies were conducted solely with Phe-PheNH$_2$. A minor modification of the method used to prepare nitrated protein was made in the case of binding studies of Abu-TyrNH$_2$. This is a weakly binding peptide (*26*), for which calculations of binding constants can be shown to be largely independent of small errors in estimating the concentration of competent protein in the preparation. Accordingly, although the protein was affinity-purified before nitration, the final nitrated product was not affinity-purified for binding studies with Abu-TyrNH$_2$. Control studies of the binding of this peptide to nitrated wild-type BNP-I gave identical results with affinity-purified and non-affinity-purified nitrated protein.

Binding Constant Calculations. The linearity of a neurophysin Scatchard plot depends on the protein concentration and dimerization constant (*25*). To handle nonlinear binding isotherms, we typically report experimental binding constants as the apparent constant at the midpoint ($\bar{\nu} = 0.5$) of the binding isotherm (*25*); curvature is not large in this region. Predicted binding constant values (K') for PNP-II and for BNP-I mutants similarly represent midpoint values. These values are the binding constants that would be operative if dimerization constant differences were the sole determinants of binding differences between mutant and wild-type BNP-I at the protein concentration of the experiment. That is, these are the values that would be operative if the intrinsic affinities of monomer and dimer sites in the mutant were the same as in the wild-type protein. They are calculated from theoretical curves derived using two different assumptions, both as described earlier (*25*). In one, the monomer is assumed not to bind at all, while in the second, the monomer is assumed to bind with one-tenth the affinity of the dimer; earlier attempts to fit the concentration-dependence of binding indicated that reality lies somewhere between the two assumptions (*25*). The intrinsic binding constants used to fit the theoretical curves are those of wild-type BNP-I, while the dimerization constants are those of PNP-II or the appropriate mutant. Therefore, the ratio of the observed binding constant, K, to K' represents the ratio of the intrinsic affinity of the mutant (or of PNP-II) to that of BNP-I. These ratios are given as the average calculated with the two assumptions ± the difference of each from the average.

RESULTS

Self-Association Properties of PNP-II. Earlier analytical gel-filtration studies of PNP-I at pH 6.7 indicated a molecular weight of ~27 000, which compared with an apparent molecular weight of ~15 000 for BNP-I under identical conditions (*13*). Repetition of these studies in the present work gave apparent molecular weights of 30 000 and 12 000 for the porcine and bovine proteins, respectively (data not shown), confirming the increased self-association of the porcine protein at neutral pH. The results are reasonably consistent with earlier analytical ultracentrifugation studies of PNP-II at pH 4.6, which had suggested a concentration-dependent molecular weight that reached ~30 000 at concentrations of 4 mg/mL (*12*). However, the high molecular weights obtained for PNP-II in these studies suggest that it is a trimer, not a dimer (calculated dimer and trimer molecular weights are 18 964 and 28 446, respectively), while only dimers have been demonstrated in solution for other neurophysins in the unliganded state (e.g., ref *2*). Accordingly, an equilibrium analytical ultracentrifugation study of the porcine protein was conducted at pH 6.2 (Figure 3). Molecular weights of 20 669 and 21 200 were obtained at initial loading concentrations of 0.4 and 0.12 mM, respectively, and were independent of concentration over the observable concentration range (0.05 to 0.7 mM). The results indicate that PNP-II exists as a tight dimer under the conditions used. Allowing a maximum of 10% dissociation to monomer at the lowest concentration investigated (0.05

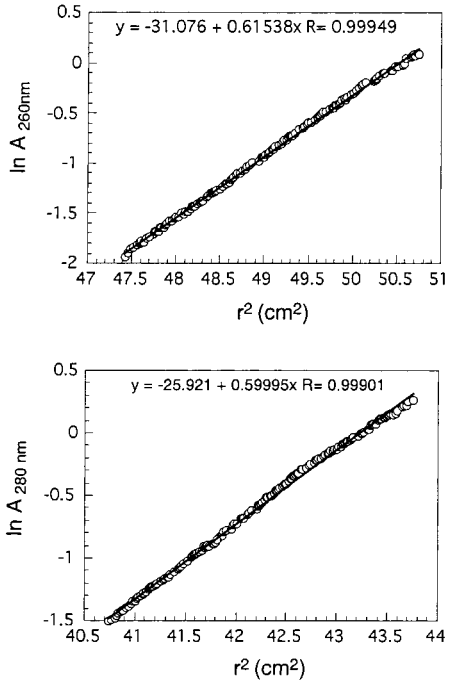

FIGURE 3: Sedimentation equilibrium analysis of porcine NP-II. The figures represent plots of the natural log of the absorbance as a function of r^2, where r is the distance between the point of measurement and the meniscus. Lower plot, data at 280 nm representing the concentration range 0.1−0.7 mM; results were obtained at a loading concentration of ~0.4 mM. Upper plot, data at 260 nm representing the concentration range 0.05−0.25 mM; results were obtained at a loading concentration of ~0.12 mM. The linearity of the data indicates a constant molecular weight over the region of observation, with the value of the molecular weight determined from the slope.

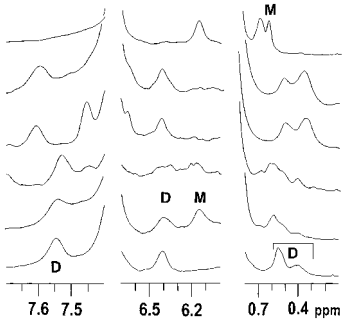

FIGURE 4: Proton NMR spectra (600 MHz) of BNP-I, PNP-II, and BNP-I mutants in regions sensitive to dimerization. Spectra were obtained in D_2O at 25 °C. In ascending order: (1) 1.6 mM BNP-I, pH 3.0, representing the all-dimer state of BNP-I; (2) 0.3 mM BNP-I, pH 6.1, representing a mixture of monomer and dimer; (3) 0.3 mM RE, pH 6.4; (4) 0.3 mM PNP-II, pH 6.1; (5) 0.15 mM RF, pH 7.0; (6) 0.3 mM DE, pH 6.2. Peaks assigned earlier to dimer and to monomer in BNP-I (*11*, *27*) are labeled D and M, respectively. Because the upfield monomer signal is indistinct in the BNP-I spectrum at pH 6.1, this peak is labeled in the DE spectrum. The signal at 7.45 ppm in the PNP-II spectrum is not routinely observed and may represent a signal from a slowly exchangeable -NH.

mM), a minimum dimerization constant of 9×10^5 M^{-1} was calculated (Table 1), which compares with 1×10^4 M^{-1} for BNP-I (e.g., Table 1) under related conditions.

One-dimensional proton NMR spectra of PNP-II were also obtained in D_2O and compared with spectra of BNP-I. Figure 4 shows regions of the spectra demonstrated earlier (*11*, *19*, *27*) to be highly sensitive to BNP-I dimerization. For example, the pH 3 spectrum of BNP-I represents all dimer

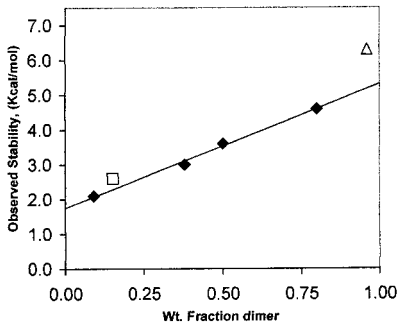

FIGURE 5: Relationship between stability at pH 6 and the weight fraction of dimer in BNP-I and selected mutants: ◆, BNP-I data obtained at 0.005, 0.05, 0.1, and 1 mM protein concentration; □, 0.1 mM EE; △, 0.1 mM RF. The dimerization constants used for BNP-I and EE are those calculated at pH 6.2 in the presence of 0.1 M ammonium acetate. The weight fraction of dimer present in the case of RF is calculated on the basis of its minimum dimerization constant (see Results).

(*27*), while the pH 6.1 spectrum represents a mixture of monomer and dimer. [Note that the differences in the regions shown are a function of dimerization and not of other pH effects (*27*).] Signals normally diagnostic of the dimeric state in BNP-I are present in the PNP-II spectra, while those characteristic of monomer are absent. Thus, the PNP-II spectra contain the 7.5−7.6 ppm dimer signal from a Phe-35 ring proton (in this case shifted slightly downfield from its location in BNP-I) and the 6.4 ppm dimer signal from a downfield α-proton, while the 6.2 ppm α-proton signal characteristic of monomer is absent (see Materials and Methods). Strong signals upfield of 0.5 ppm were present, as found only in the BNP-I dimer (*27*), but in this case shifted still further upfield. Spectra appeared identical at 0.3 and 0.06 mM concentrations (data not shown), consistent with the minimum dimerization constant estimated from the ultracentrifuge data.

Relative Stabilities of PNP-II and BNP-I and Their Effects on Folding. The stability of BNP-I to guanidine denaturation is concentration-dependent (Table 2, Figure 5), increasing linearly[2] by over 2 kcal/mol at pH 6 as the concentration is increased from 0.00 to 1 mM, and the weight fraction of dimer increases from 9% to 80%. In accord with this, the stronger self-association of PNP-II than of BNP-I is manifest in guanidine denaturation studies (Table 2, Figure 5) as a stability increase of 2.8 kcal/mol when the two proteins are compared at concentrations of 0.1 mM. Values of m derived from the data are also higher for PNP-II than for BNP-I at equivalent concentrations (Table 2), which is consistent with a greater exposure of surface area upon denaturation of the porcine protein.

Mature bovine neurophysins are metastable with respect to their disulfide pairs (*6*, *8*, *28*, *29*). The native state of BNP-II is ~1 kcal/mol less stable than a disulfide-scrambled state (*8*), while the native and scrambled states of BNP-I are of approximately equal energies (R. Deeb and E. Breslow, unpublished studies). Efficient refolding of these proteins from the disulfide-reduced state therefore depends on the presence of ligand peptides to stabilize the native structure (*8*, *28*). If folding is strictly controlled thermodynamically

[2] The linear relationship seen here between stability and weight fraction dimer is empirical and is not obviously predicted by denaturation considerations.

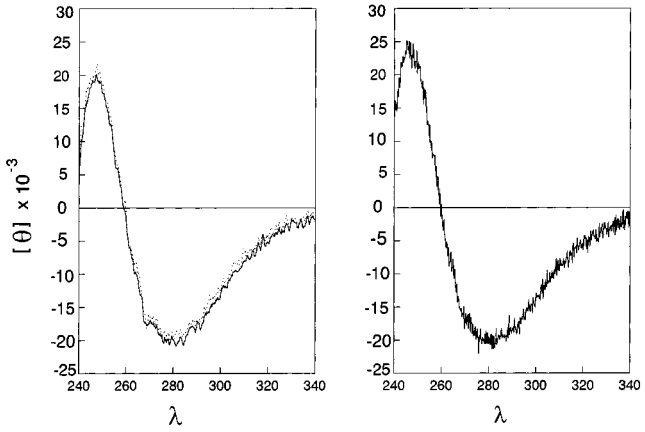

FIGURE 6: Comparison of the near-ultraviolet CD spectra of the products obtained by refolding a sample of reduced PNP-II in the presence and absence of Phe-TyrNH$_2$. Left: solid line, protein refolded in the absence of peptide; dotted line, protein refolded in the presence of peptide. Right: spectrum of purified folded PNP-II. Results are reported as molar ellipticities.

in NP, the extra stability of PNP-II relative to BNP-I should be sufficient to allow its efficient refolding from the reduced state in the absence of ligand peptides. This was shown to be the case. A sample of folded PNP-II was completely reduced, and aliquots were allowed to reoxidize in either the presence or absence of ligand peptide. The protein was separated from all ligand and other reagents by gel filtration at low pH, but it was not otherwise purified. Figure 6 compares the disulfide CD spectra of the protein products obtained in the absence and presence of ligand peptide. The disulfide CD spectrum is known to be highly sensitive to the correct folding of the protein. Incorrect folding leads to loss of the positive 245 nm band and to the shifting and changing of the shape of the 280 nm band (*29*). As evidenced from Figure 6, peptide has no significant influence on the final product. However, small spectral differences between the final product and that of the starting unreduced protein can be seen in both cases and are attributed to the small fraction of irreversibly damaged protein shown earlier to be produced during reduction and/or refolding (*28*).

Relative Binding Properties of PNP-II and BNP-I. The higher dimerization constant of PNP-II than of BNP-I might also be expected to result in stronger binding by the porcine protein at concentrations representing a higher weight fraction of dimer in the porcine protein; binding to a dimer site is estimated to be ≥10 times stronger than that to a monomer site (*25*). However, comparison of the binding affinities of PNP-II and BNP-I at pH 6.2 for the dipeptide Phe-PheNH$_2$, each at a protein concentration of 0.05 mM (unliganded PNP-II is all dimer and BNP-I is 38% dimer by weight at this concentration), indicated no significant difference in their binding (Figure 7 , Table 3) despite their large difference in self-association. This is most clearly seen in Figure 7 by comparison of the observed binding isotherms for the two proteins with results predicted based on the differences in their dimerization. The observed binding data for BNP-I are shown to be approximated by a theoretical curve calculated assuming no binding by monomer, an intrinsic binding constant for each dimer site of 24×10^3 M^{-1}, and a dimerization constant in the unliganded state of 1×10^4 M^{-1}. (The calculated intrinsic binding constant for a dimer site falls to $\sim 20 \times 10^3$ M^{-1} if the monomer is allowed to bind with 10% the affinity of a dimer site.) However, the PNP-II binding data give a binding constant per dimer site of $\sim 11 \times 10^3$ M^{-1}, indicating an intrinsic affinity approximately one-half that of a BNP-I dimer (theoretical curve for PNP-II). The ratio of the experimental binding constant, *K*, to that predicted by its dimerization properties, *K*′, is reported in Table 3. A competition study of the relative abilities of BNP-I and PNP-II to compete with nitrated bovine NP-II for oxytocin led to similar conclusions about their relative binding affinities (data not shown).

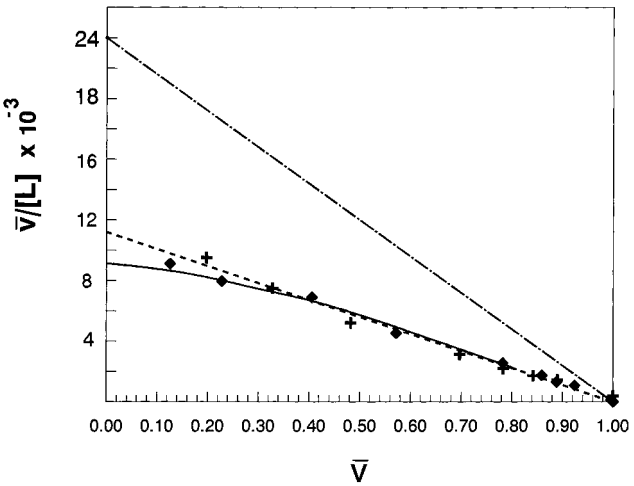

FIGURE 7: Comparison of the binding of Phe-PheNH$_2$ by 0.05 mM BNP-I and 0.05 mM PNP-II at pH 6.2, as determined by fluorescence spectroscopy: ◆, BNP-I data; +, PNP-II data; − − −, straight line fit of the PNP-II data; —, theoretical binding curve for BNP-I calculated using a dimerization constant, in the unliganded state, of 1×10^4 M^{-1} and assuming that only dimer binds with an intrinsic binding constant for each site of 24 000 M^{-1}; − · − · −, theoretical binding curve (straight line) for PNP-II, assuming an intrinsic binding constant per dimer site of 24 000 M^{-1}.

Table 3: Peptide-Binding Constants of BNP-I, PNP-II, and Mutant Neurophysins at 25 °C[a]

	exptl binding constant (M^{-1})		*K*/*K*′	
	Phe-PheNH$_2$	Abu-TyrNH$_2$	Phe-PheNH$_2$	Abu-TyrNH$_2$
BNP-I	1.1×10^4	1.7×10^3	1.0	1.0
PNP-II	1.1×10^4	ND	0.5 (±.05)	ND
RF mutant	1.1×10^4	9.5×10^2	0.5 (±.05)	0.32 (±0.01)
RE mutant	4.0×10^3	3.4×10^2	≤0.4[b]	≤0.2[b]
DE mutant	7.0×10^3	6.0×10^2	1.4 (±0.1)	0.65 (±0.05)
EE mutant	8.7×10^3 [c]	$6\ (\pm 1) \times 10^2$	1.5 (±0.05)	0.65 (±0.05)

[a] Binding constants for Phe-PheNH$_2$ were determined by fluorescence at a protein concentration of 0.05 mM, except as indicated otherwise. Data for Abu-TyrNH$_2$ were determined by CD using nitrated protein at a concentration of 0.1 mM. All studies were conducted at pH 6.2 in 0.1 M ammonium acetate containing 2 mM Mes. *K*/*K*′ is the ratio of the experimental binding constant (*K*) to the theoretical binding constant (*K*′), where *K*′ is calculated from BNP-I binding data with corrections for differences in dimerization constants using two different assumptions, as described in Materials and Methods. The value of *K*/*K*′ shown is the average of the two methods of calculation ± the difference from the mean of each. [b] Because of the uncertain magnitude of the RE dimerization constant, it was assumed to be the same as that of wild-type BNP-I for these calculations. To the extent that this is an underestimate of its dimerization constant, the values of *K*/*K*′ given are minimum values. Note that in this case, the theoretical *K*′ is simply the observed binding constant of the wild-type protein. [c] Protein concentration equals 0.07 mM.

Localization of the Source of the Increased Stability and Dimerization of PNP-II, and of Its Altered Binding, to the Substitutions at Positions 80 and 81. To determine the extent to which differences in the properties of BNP-I and PNP-II were due to differences at positions 80 and 81, residues 80 and 81 of BNP-I were mutated to Arg and Phe, respectively, as in PNP-II, to give the RF mutant. Stability studies of the RF mutant (Table 2) indicated an increase in stability relative to BNP-I within an experimental error of that seen in PNP-II. Consistent with this, NMR spectra of the RF mutant at pH 7 (Figure 4) exhibited the identical dimerization-sensitive signals seen in the spectra of PNP-II, with the same chemical shifts and the absence of signals diagnostic of the monomer. In the analytical ultracentrifuge at pH 6, the RF bovine NP-I mutant behaved as a single species with a calculated molecular weight of 22 300 over the observed concentration range 0.01−0.5 mM. If one assumes that the mutant is a dimer (theoretical molecular weights for dimer and trimer are ~19 000 and 28 500, respectively) and that 10% monomer would not be detected, a minimum dimerization constant of 3.5×10^6 M^{-1} is calculated (Table 1).

To further define factors contributing to the stability difference between the RF mutant and the wild-type protein, the stabilities of the two proteins were compared at pH 3.5 (Table 2). The dimerization constant of native BNP-I is markedly increased at low pH (*21*, *27*). NMR studies (*21*) indicate that it is 65 times greater at pH 3.5 in phosphate buffer than at pH 6 (Table 1), a fact we tentatively attribute to protonation of Glu-81. [Glu-81 is the only interface carboxyl group that is not analogous to one in BNP-II, and BNP-II dimerization does not significantly change at low pH (*2*, *21*).] Because Glu-81 is substituted in the RF mutant, the difference in stability between the native protein and the RF mutant is expected to diminish at pH 3.5 to the extent that their dimerization properties become more equivalent. The results show that the difference of 2.8 kcal/mol at pH 6 and 0.1 mM concentration is reduced to 2.3 kcal/mol at pH 3.5, consistent with a role for dimerization in the increased stability of the RF mutant, but suggesting that other factors might also be involved (see Discussion). Results at low pH with PNP-II were within the experimental error of those obtained with the RF mutant (Table 2).

As with PNP-II, the extra stability of the RF mutant permitted it to fold efficiently from the reduced state in the absence of added peptide. Using CD to monitor disulfide optical activity (Figure 8), the course of folding was monitored at pH 8 in the presence of air and β-mercaptoethanol (see Materials and Methods). Consistent with the behavior of BNP-II (*8*), folding did not proceed in an all-or-none manner. Evidence of rapid formation of a state in which all the disulfides are probably not properly paired is seen in the more rapid development of intensity in the 280 nm disulfide band than in the positive 245 nm band, the 280 nm band shifting to longer wavelengths during completion of the development of the 245 nm band. For comparison, a comparable study of refolding of wild-type BNP-I in the absence of added peptide is also shown (Figure 8), the results illustrating the inability of BNP-I to attain the native conformation under these conditions.

Two types of binding studies were conducted with the RF mutant (Table 3). Affinities of the unmodified protein for Phe-PheNH$_2$ were determined by fluorescence using unmodified protein, giving results identical to those reported above for PNP-II. That is, no significant differences in the observed binding by the wild-type protein and RF mutant were seen, despite differences in dimerization, indicating an intrinsic binding affinity 50% of that of the wild-type protein and demonstrating that residues 80−81 are the sole source of the binding affinity difference between PNP-II and wild-type BNP-I. However, the observed affinity of the nitrated RF mutant for the peptide Abu-TyrNH$_2$ was significantly less than that of the wild-type protein, indicating an intrinsic affinity 30% of that of the wild-type protein for this peptide. The differences in the results obtained with the two peptides are not due to the different binding methodologies used. Control CD studies of the relative binding of the wild-type protein and RF mutant to Phe-PheNH$_2$ using nitrated protein gave results analogous to those obtained by fluorescence. The results indicate an effect of the RF mutation both on absolute affinities and on the relative binding affinity for Phe-PheNH$_2$ and Abu-TyrNH$_2$.

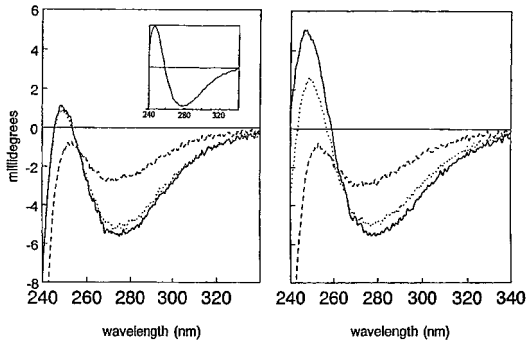

FIGURE 8: Refolding of wild-type BNP-I and its RF mutant in the absence of peptide, as monitored by CD at 25 °C. The reduced protein at pH 3 in 0.1 M acetic acid was adjusted to pH 8 with saturated Tris in the presence of β-mercaptoethanol and EDTA (see Materials and Methods) and allowed to stir in air. CD spectra were then acquired as a function of time. Left: refolding of the wild-type protein; dashed line, initial reading; dotted line, after 5 h; solid line, after 24 h. Inset is the corresponding spectrum of the native protein. Right: refolding of the RF mutant; dashed line, initial reading; dotted line, after 45 min; solid line, after 4 h. No further changes were seen in the spectrum of the RF mutant after 4 h. Note that disulfides are the only optically active chromophores in these spectra and that the initial spectra in both cases indicate that significant disulfide formation occurs within several minutes of adjusting the reduced protein to pH 8.

Effects of the Single Mutation of His-80 to Arg. Studies were also conducted of the mutant containing the His to Arg mutation at position 80 but retaining Glu at position 81 (RE mutant). The results provide potential insights into the binding behavior of the RF mutant.

NMR spectra of the RE mutant (e.g., see Figure 4) indicate a dimerization constant markedly lower than that of the RF mutant but higher than that of the wild-type protein. Ambiguities arise because NMR spectra of RE exhibit subtle differences from those of the wild-type protein not attributable to different signals from residue 80. The relative intensities of the monomer and dimer signals at 6.2 and 6.4 ppm suggest a dimerization constant (Table 1) approximately 6 times that of BNP-I when adjustments for pH differences are made, although these signals are very poorly defined in this mutant, perhaps because of exchange processes. While the intensity of the 7.57 ppm dimer signal might point to a still-higher value, only the lower estimate is consistent with

the most-upfield region of the spectrum (Figure 4) and with preliminary studies of the pH dependence of binding (not shown), suggesting that the 7.57 ppm signal contains contributions from more than one proton in this mutant. The results indicate the importance of Phe-81 to the strong dimerization of the RF mutant.

In addition to its NMR spectrum, CD spectra of the RE mutant suggest a possibly atypical conformation in the unliganded state. The height of the positive 245 nm band relative to that of the negative 280 nm band (245/280 nm ratio) is only 50−60% that of the wild-type protein (cf., see Figure 8) and the other mutants (data not shown). This effect is not due to charge alone, because it is absent in the RF mutant. Additionally, the 350 nm nitrotyrosine CD signal in nitrated RE, although normal in the liganded state, is abnormally weak in the unliganded state, having only one-third the intensity of that seen in the nitrated derivatives of the wild-type protein or its other mutants (data not shown). Because Tyr-49 is clearly distant from residue 80 (*3*, *4*), the results suggest long-range structural effects of this mutation. These spectral abnormalities are not affected by dilution to very low concentrations, indicating that they represent intrasubunit effects.

Binding studies for RE (Table 3) gave an apparent binding constant for Phe-PheNH_2 approximately 40% that of wild-type protein, representing a maximum (see Table 3 footnote) of 40% of the intrinsic affinity of the wild-type protein. The intrinsic affinity for Abu-TyrNH_2 was maximally 20% that of the wild-type protein. The results strongly suggest that the diminished binding affinity and altered binding specificity of the RF mutant reflect the substitution of Arg for His at position 80.

Reduction of Dimerization by Mutation of Residue 80 to Asp or Glu; Properties of the DE and EE Mutants. An apparent role of a positive charge on His-80 in facilitating dimerization of BNP-I[3] and negative effects of His-80 carboxymethylation on dimerization (*11*) suggested that replacement of His-80 by a negatively charged residue would reduce dimerization. NMR studies confirmed that changing residue 80 of BNP-I to Asp or Glu reduced dimerization by a factor of ~10 when the wild-type and mutant proteins were compared under equivalent conditions (Table 1). This is shown specifically for the DE mutant in Figure 4. The absence of dimer is evidenced by the absence of the 7.57 ppm Phe proton signal; the shift of the most-downfield α-proton signal from ~6.4 ppm, representative of dimer, to ~6.2 ppm, representative of monomer (*11*); and the chemical shift of the most-upfield signals, which on average are located >0.1 ppm downfield from the most-upfield signals in the wild-type BNP-I dimer, as observed earlier for the change from dimer to monomer in the wild-type protein (*27*). Signal line width is also sharper than in, for example, the dimeric

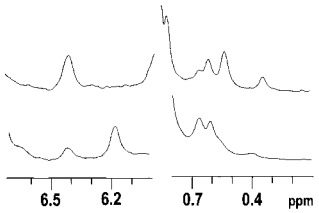

FIGURE 9: Effect of peptide binding on the 600 MHz NMR spectrum of the EE mutant. Lower spectrum: EE alone (0.54 mM), pH 6.18 in D_2O containing 50 mM NaCl. Upper spectrum: same sample, but after addition of 5 mM Phe-PheNH_2, final pH 6.13. Peptide leads to loss of the 6.2 ppm monomer band and an increase in intensity of the 6.4 ppm dimer band. Changes in the upfield region are typical of those associated with formation of bound dimer (cf., ref *18*).

RF mutant. As shown for the EE mutant (Table 2), the reduced dimerization constant is accompanied by a 0.4 kcal/mol lower stability than that of the wild-type protein at the same concentration, the stability approximating that of the wild-type protein at equivalent weight fractions of dimer (Figure 5).

The dimerization constants of the DE and EE mutants increase upon peptide binding, indicating that mutant behavior parallels that of the wild-type protein, at least qualitatively, in this respect. As shown in Figure 9 for EE, saturation with Phe-PheNH_2 leads to loss of the 6.2 ppm monomer peak and its substitution by the 6.4 ppm dimer signal (the chemical shift of the 6.4 ppm dimer signal is independent of binding) associated with changes in the upfield region to give a spectrum characteristic (e.g., ref *18*) of bound dimer. Also like the wild-type protein, EE dimerization exhibited a strong pH dependence in the unliganded state (Table 1), in this case decreasing by a factor of more than 20 between pH 6.1 and 7.5 and indicating the importance of carboxyl protonation to dimer formation.

The reduced dimerization constants of the DE and EE mutants are ambiguously manifest in peptide-binding studies (Table 3). Calculated values of K/K' indicate intrinsic dimerization-corrected affinities for Phe-PheNH_2 that are 40−50% higher than for the wild-type protein, contrasting in direction and magnitude to results obtained with PNP-II, RE, and RF. Intrinsic affinities for Abu-TyrNH_2 are only 65% of predicted values. The difference between the two peptides is, therefore, qualitatively similar to that seen with the other mutants.

DISCUSSION

We show here that mutation of residues 80 and 81 at the subunit interface allows NP dimerization to be manipulated over a wide range and has consequences that are directly associated with the quantitative change in dimerization and consequences that are independent of this change. Changes in dimerization are associated with changes in stability. Of particular significance is that the increase in stability provided by the RF mutation confers on BNP-I the ability to fold in the absence of ligand peptide. This is consistent with the thermodynamic control of folding in this system, first demonstrated for BNP-II folding in the presence of non-sulfur-containing ligand dipeptides (*8*), and also emphasizes the atypical nature of the folding problems encountered in the presence of the natural ligand oxytocin. Refolding in vitro of either reduced, denatured, mature BNP-II in the presence

[3] A role of His-80 protonation in dimerization (additional to that of carboxyl titration) was suggested by the pH dependence of dimerization of BNP-I throughout the pH region 6.5−8 (*11*). Preliminary studies of the pH dependence of the dimerization of the RE mutant show a reduction in dimerization between pH 6 and 7 that can only be attributed to carboxyl titration and which, therefore, is likely to contribute to pH effects in this region in the wild-type protein. No evidence of a contribution of carboxyl titration is seen above pH 7, suggesting that changes between pH 7 and 8 in the wild-type protein primarily reflect His-80 titration.

of oxytocin (*8*) or the common precursor of oxytocin and BNP-I (*18*) is less efficient than predicted by stability considerations due to disulfide cross-linking problems generated by the unstable oxytocin disulfide (*18*).

The generation of neurophysins with low dimerization constants on the one hand and with self-folding properties on the other has the potential to facilitate insights into several aspects of NP function that have otherwise been difficult to explore. The dimerization constants of the DE and EE mutants are sufficiently low to permit structural and functional investigation of the NP monomeric state in solution. This is important to an understanding of the relationship between dimerization and ligand binding in this system, and while it is known that unliganded monomers and dimers differ in structure (e.g., ref *19*), the nature of these differences is uncertain. The self-folding properties of the RF mutant separate the process of folding from that of ligand binding and therefore should have particular applicability to the elucidation of precursor targeting mechanisms. For example, they potentially allow determination of the extent to which the targeting failure associated with deletion of the hormone sequence of the precursor (*30*) and the pathology resulting from mutations at the hormone-binding site of NP in diabetes insipidus (*31*) solely reflect folding problems generated by insufficient precursor stability in the absence of hormone−NP interaction or involve other issues of structure or recognition.

It is relevant to point out, however, that factors other than dimerization might contribute to the observed stability differences, as particularly suggested by the comparison of RF with the wild-type protein. At pH 6, the stability difference between RF and wild-type BNP-I is 2.8 kcal/mol at 0.1 mM concentration (Table 2), which is reasonably consistent with the large difference in their dimerization under these conditions (e.g., Figure 5). At low pH, the difference between the two proteins is expected to diminish as a consequence of the increased dimerization of the wild-type protein (see Results). However, the observed reduction of 0.5 kcal/mol in this difference (Table 2) is significantly less than the expected reduction of 2.1 kcal/mol calculated from the difference in the free energy of dimerization of the wild-type protein at the two pH values (see Materials and Methods). While alternative explanations of the relatively small effect of pH are possible, the results suggest that stability differences between the two proteins might in part reflect differences in subunit stability that are independent of dimerization and which derive from changes in intrachain interactions that alter subunit conformation and secondarily affect dimerization.

The results also show that mutation of residues 80 and 81 leads to effects on binding affinity and specificity that are independent of quantitative changes in dimerization, that is, effects on the intrinsic affinities of the dimer and/or monomer. These effects are most clearly evident in the RE and RF mutants, where they are attributed to the substitution of Arg for His at position 80. Some of the effects manifest in RE may result from an atypical conformation, but the effects seen in the RF mutant, which does not manifest the same spectral properties as RE, are similar in direction. The substitution of Arg for His significantly reduces binding affinity for both Phe-PheNH_2 and Abu-TyrNH_2 and alters the relative binding of the two peptides, despite increases in dimerization constant. While the effects on binding affinity are less than an order of magnitude, they are of particular interest because they do not appear to be random. PNP-II differs from wild-type BNP-I not only in positions 80 and 81 but also in four other residues (Figure 2). One of these (residue 9) is relatively close to the binding site and another (residue 64) is immediately adjacent to the site of a mutation in human vasopressin-associated NP which is associated with diabetes insipidus (*32*). The identity of the binding affinities of PNP-II and RF for Phe-PheNH_2 suggests both a specific role for residues 80 and 81 and the absence of a role for these other residues in modulating binding affinity.

The effects on intrinsic binding affinities associated with the RE and RF mutants are consistent with evidence that deprotonation of His-80 increases affinity (discussed in ref *18*) and suggest that the magnitude of positive charge at position 80 correlates inversely with binding affinity. Results obtained with DE and EE suggest that a negative charge increases affinity, at least for Phe-PheNH_2, although the effects here are smaller. Mutation-induced changes in specificity have a parallel in data suggesting that the relative affinities of BNP-I and -II for different peptides are nonidentical (25), the two proteins differing at positions 80 and 81, albeit also at a number of other positions (Figure 2). A structural basis for the mutation-induced changes in affinity and specificity is suggested by the demonstration that peptide binding is accompanied by perturbation of His-80 (*14*, *33*), indicating that binding to BNP-I is associated with conformational change in the carboxyl domain segment of the interface. The energetics of this change will necessarily contribute to the overall thermodynamics of binding and will depend on the relative interactions of interface residues in liganded and unliganded states, which are in turn a reflection of the composition of the interface. That is, stronger interactions of Arg-80 than of His-80 in the unliganded state, which need to be broken in the liganded state, will reduce the binding affinity of mutants with Arg at this position. Similarly, differences in the conformational rearrangements needed to accommodate different peptides represent a potential basis for the effects of mutations in this region on binding specificity. The changes in affinity and specificity found here therefore provide evidence of a direct thermodynamic link between the binding site and the carboxyl domain segment of the subunit interface and are of potential relevance to an understanding of the structural basis of the thermodynamic coupling between NP binding and self-association.

ACKNOWLEDGMENT

We are particularly grateful to Art Villafania for excellent and critical technical assistance, to Ayna N. Alfadhli for contributions to NMR investigations, and to Professor Min Lu of this Department for the analytical ultracentrifuge studies.

REFERENCES

1. Nicolas, P., Camier, M., Dessen, P., and Cohen, P. (1976) *J. Biol. Chem. 251*, 3965−3971.
2. Nicolas, P., Batelier, G., Rholam, M., and Cohen, P. (1980) *Biochemistry 19*, 3565−3573.
3. Chen, L., Rose, J. P., Breslow, E., Yang, D., Chang, W. R., Furey, W. F., Jr., Sax, M., and Wang, B.-C. (1991) *Proc. Natl. Acad. Sci. U.S.A. 88*, 4240−4244.

4. Rose, J. P., Wu, C. K., Hsaio, C. D, Breslow, E., and Wang, B.-C. (1996) *Nat. Struct. Biol. 3*, 163−169.
5. Wu, C. K., Rose, J. P., Zheng, C., Breslow, E., and Wang, B.-C. (1996) *Acta Crystallogr., Sect. D: Biol. Crystallogr. 52*, 946−949.
6. Breslow, E., and Burman, S. (1990) *Adv. Enzymol. 63*, 1−67.
7. Chaiken, I. M., Tamaoki, H., Brownstein, M., and Gainer, H. (1983) *FEBS Lett. 164*, 361−365.
8. Deeb, R., and Breslow, E. (1996) *Biochemistry 35*, 864−873.
9. Chauvet, M. T., Hurpet, D., Chauvet, J., and Acher, R. (1983) *Proc. Natl. Acad. Sci. U.S.A. 80*, 2839−2843.
10. Abercrombie, D. M., Kanmera, T., Angal, S., Tamaoki, H., and Chaiken, I. M. (1984) *Int. J. Pept. Protein Res. 24*, 218−232.
11. Breslow, E., Mishra, P. K., Huang, H.-b., and Bothner-by, A. (1992) *Biochemistry 31*, 11397−11404.
12. Uttenthal, L. O., and Hope, D. B. (1970) *Biochem. J. 116*, 899−909.
13. Breslow, E., LaBorde, T., Saayman, H. S., Oelofsen, W., and Naude, R. J. (1992) *Int. J. Pept. Protein Res. 39*, 388−396.
14. Virmani-Sardana, V., and Breslow, E. (1983) *Int. J. Pept. Protein Res. 21*, 182−189.
15. Rabbani, L., Pagnozzi. M., Chang, P., and Breslow, E. (1982) *Biochemistry 21*, 817−826.
16. Breslow, E., Aanning, H. L., Abrash, L., and Schmir, M. (1971) *J. Biol. Chem. 246*, 5179−5188.
17. Sardana, V., and Breslow, E. (1984) *J. Biol. Chem. 259*, 3669−3679.
18. Eubanks, S., Lu, M., Peyton, D., and Breslow, E. (1999) *Biochemistry 38*, 13530−13541.
19. Breslow, E., Sardana, V., Deeb, R., Barbar, E., and Peyton, D. H. (1995) *Biochemistry 34*, 2137−2147.
20. Zheng, C., Peyton, D., and Breslow, E. (1997) *J. Pept. Protein Res. 50*, 199−209.
21. Zheng, C., Cahill, S., and Breslow, E. (1996) *Biochemistry 35*, 11763−11772.
22. Whittaker, B. A., and Allewell, N. M. (1984) *Arch. Biochem. Biophys. 234*, 585−590.
23. Neet, K. E., and Timm, D. E. (1994) *Protein Sci. 3*, 2167−2174.
24. Sur, S., Rabbani, L. D., Libman, L., and Breslow, E. (1979) *Biochemistry 18*, 1026−1036.
25. Breslow, E., LaBorde, T., Bamezai, S., and Scarlata, S. (1991) *Biochemistry 30*, 7990−8000.
26. Breslow, E., and Gargiulo, P. (1977) *Biochemistry 16*, 3397−3406.
27. Peyton, D., Sardana, V., and Breslow, E. (1986) *Biochemistry 25*, 6579−6586.
28. Huang, H.-b., and Breslow, E. (1992) *J. Biol. Chem. 267*, 6750−6756.
29. Menendez-Botet, C. J., and Breslow, E. (1975) *Biochemistry 14*, 3825−3835.
30. de Bree, F. M., and Burbach, J. P. (1998) *Cell Mol. Neurobiol. 18*, 173−191.
31. Rittig, S., Robertson, G. L., Siggaard, C., Kovacs, L., Gregersen, N., Nyborg, J., and Pedersen, E. B. (1996) *Am. J. Hum. Genet. 58*, 107−117.
32. Rauch, F., Lenzner, C., Nurnberg, P., Frommel, C., and Vetter, U. (1996) *Clin. Endocrinol. 44*, 45−51.
33. Griffin, J., Cohen, J. S., Cohen, P., and Camier, M. (1975) *J. Pharm. Sci. 64*, 507−511.
34. Pace, C. N. (1975) *Crit. Rev. Biochem. 3*, 1−43.

BI0001527